

DOI: 10.1002/ange.200602479

**Control of  $\pi$ -Electron Rotation in Chiral Aromatic Molecules by Nonhelical Laser Pulses\*\****Manabu Kanno, Hirohiko Kono, and Yuichi Fujimura\**

The control of electron dynamics in molecules or molecular assemblies by irradiation is a fascinating research field.<sup>[1,2]</sup> Control of the photocurrents of molecular devices in the ultrashort time regime is essential for nanotechnology. However, fundamental issues remain to be clarified for the manipulation of electron motions, especially in large molecules such as those having aromatic rings. Aromatic molecules are characterized by delocalized  $\pi$  electrons that can in principle be controlled using UV/Vis light. One of the issues is how to control their rotation direction (ring current) using ultrashort UV/Vis laser pulses. It is unclear whether  $\pi$  electrons can be rotated along an aromatic ring by a nonhelical, linearly polarized laser pulse, though  $\pi$ -electron rotation can be performed using a circularly polarized laser pulse.<sup>[3]</sup> In the latter case, the rotation direction is predetermined by the applied pulse. If  $\pi$ -electron rotation is induced by a linearly polarized laser pulse, the rotation direction should be intrinsic to the molecule of interest because a nonhelical photon has no angular momentum. Therefore, its electron dynamics should reflect the asymmetry of the molecule itself.

We show here that the polarization direction of a linearly polarized laser pulse determines the initial direction of  $\pi$ -electron rotation in a chiral aromatic molecule. We then propose a pump–dump control method for determining

[\*] M. Kanno, Prof. H. Kono, Prof. Y. Fujimura  
Department of Chemistry  
Graduate School of Science, Tohoku University  
Sendai 980-8578 (Japan)  
Fax: (+81) 22-795-7715  
E-mail: fujimurayuichi@mail.tains.tohoku.ac.jp

[\*\*] M.K. is grateful to Dr. K. Hoki, Dr. Y. Teranishi, and Prof. T. Kato for fruitful discussions and acknowledges financial support from a JSPS Research Fellowship for Young Scientists (No. 18-5252). This work was partly supported by a JSPS Research Grant (No. 17350004).



Supporting information for this article is available on the WWW under <http://www.angewandte.org> or from the author.

unidirectional rotation of  $\pi$  electrons in a chiral aromatic molecule.

A chiral aromatic molecule with a six-membered ring, 2,5-dichloro[ $n$ ](3,6)pyrazinophane (DCP;  $n$  specifies the length of the ethylene bridge  $(\text{CH}_2)_n$ ), was chosen (Figure 1). DCP

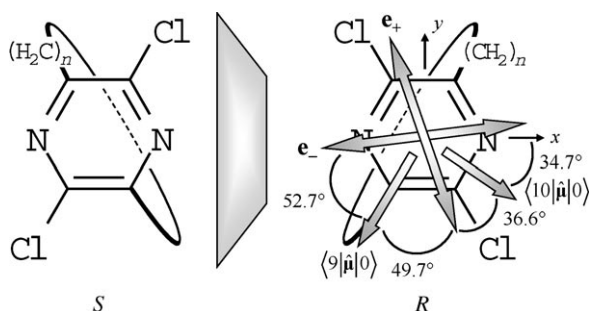


**Figure 1.** *S* and *R* enantiomers of DCP. The directions of transition dipole moments  $\langle 9|\hat{\mu}|0\rangle$  and  $\langle 10|\hat{\mu}|0\rangle$  of an *R* enantiomer are shown as well as those of photon polarization vectors  $\mathbf{e}_{\pm}$  defined as  $\langle 9|\hat{\mu}|0\rangle \mathbf{e}_{\pm} = \pm \langle 10|\hat{\mu}|0\rangle \mathbf{e}_{\pm}$ . The magnitudes of  $\langle 9|\hat{\mu}|0\rangle$  and  $\langle 10|\hat{\mu}|0\rangle$  are  $2.02\ e a_0$  and  $1.63\ e a_0$ , respectively.

has quasi-degenerate  $\pi$ -electronic excited states. We use a coherent superposition of the quasi-degenerate states for controlling temporal behavior of an electron wave packet. The length of the ethylene bridge  $(\text{CH}_2)_n$  is restricted ( $n \lesssim 10$ ) to avoid conversion between enantiomers through free rotation of the aromatic ring. We assume that the molecule is fixed to a surface by the ethylene bridge. Since the period of  $\pi$ -electron rotation is shorter by one order than the vibration periods of nuclei, the nuclei in the molecule are treated as being fixed.

The Hamiltonian of an aromatic molecule interacting with a classical laser field  $\epsilon(t)$  is expressed in the dipole approximation as Equation (1), where  $\hat{H}_{\pi}$  is the effective  $\pi$ -electronic Hamiltonian and  $\hat{\mu}$  is the electric dipole moment operator.

$$\hat{H}(t) = \hat{H}_{\pi} - \hat{\mu} \epsilon(t) \quad (1)$$

For  $\hat{H}_{\pi}$  we use the semiempirical Pariser–Parr–Pople (PPP) model, which has been demonstrated to reproduce various optical properties of  $\pi$ -conjugated systems with a proper choice of parameters.<sup>[4,5]</sup> The effect of the nonaromatic ethylene bridge is ignored in the PPP model. Then, DCP is regarded as being of  $C_{2h}$  symmetry and having eight  $p_z$  orbitals and 10  $\pi$  electrons in this description of  $\pi$ -electron dynamics. Parameters for one-electron energies and Coulomb repulsions are set as employed for linear polyenes,<sup>[5]</sup> and the energetic properties of Cl and N atoms are introduced as originally formulated by Streitwieser.<sup>[6]</sup> The aromatic ring forms a planar structure, and we simply assume that the C–C and C–N bond lengths are 1.40 Å, the C–Cl bond length is 1.80 Å, and  $\angle(\text{N–C–Cl}) = 120^\circ$ .

The time-dependent Schrödinger equation (TDSE) [Eq. (2)] can be solved by expanding  $|\Psi(t)\rangle$  in terms of 136 singlet eigenstates of  $\hat{H}_{\pi}$  obtained at the level of singly and doubly excited configuration interaction (SDCI), that is,

$|\Psi(t)\rangle = \sum_{k=0}^{135} c_k(t) e^{-iE_k t/\hbar} |k\rangle$ , where  $|0\rangle = |1^1A_g\rangle$  is the ground state.<sup>[7]</sup> By inserting the expanded form of  $|\Psi(t)\rangle$  into the TDSE [Eq. (2)], we derive the coupled equations of motion for the expansion coefficients  $\{c_k(t)\}$ .

$$i\hbar \frac{\partial}{\partial t} |\Psi(t)\rangle = \hat{H}(t) |\Psi(t)\rangle \quad (2)$$

In this model,  $\pi$ -electron rotation can be quantified by the momentum expectation value  $p(t) \equiv \langle \Psi(t) | \hat{p} | \Psi(t) \rangle$ , where  $\hat{p}$  is defined using the momentum of complex molecular orbitals for a circular path along an aromatic ring.<sup>[7]</sup> Here, in a circular motion of a particle, angular velocity of the particle is equivalent to its velocity divided by the radius of the circle. Thus, we also define the rotational angle of  $\pi$  electrons,  $\theta(t)$ , in Equation (3), where  $b$  is the radius of the ring. The expectation values  $p(t)$  and  $\theta(t)$  are used as measures of  $\pi$ -electron rotation.

$$\theta(t) \equiv \frac{1}{m_e b} \int_0^t d\tau p(\tau) \quad (3)$$

DCP has quasi-degenerate  $\pi$ -electronic excited states  $|9\rangle = |5^1B_u\rangle$  and  $|10\rangle = |6^1B_u\rangle$  with the energy gap  $2\Delta E \equiv E_{10} - E_9 = 0.105\text{ eV}$  ( $E_9 - E_0 = 7.66\text{ eV}$ ). The transition dipole moments  $\langle 9|\hat{\mu}|0\rangle$  and  $\langle 10|\hat{\mu}|0\rangle$  of an *R* enantiomer of DCP are illustrated in Figure 1, and those of an *S* enantiomer are their mirror images. Linear combinations of  $|9\rangle$  and  $|10\rangle$  give the approximate eigenstates of the angular momentum operator  $\ell = \hbar \hat{p}$ , denoted as  $|+\rangle$  and  $|-\rangle$ , where  $\langle \pm | \ell | \pm \rangle = \pm 0.862\hbar$ : For an *R* enantiomer this is described by Equation (4), and for an *S* enantiomer, the sign  $\pm$  on the right-hand side of Equation (4) is replaced by  $\mp$ .  $\pi$  Electrons with positive (negative) angular momentum travel counter-clockwise (clockwise) around the ring in Figure 1.

$$|\pm\rangle = 2^{-1/2} (|9\rangle \pm i|10\rangle) \quad (4)$$

We now design a linearly polarized laser pulse  $\epsilon(t)$  to generate predominantly either  $|+\rangle$  or  $|-\rangle$ . First, the central frequency  $\omega$  of  $\epsilon(t)$  is determined as  $\omega = (E_9 + \Delta E - E_0)/\hbar$ . Next, the polarization direction of  $\epsilon(t)$  is determined by its alignment relative to  $\langle 9|\hat{\mu}|0\rangle$  and  $\langle 10|\hat{\mu}|0\rangle$ . This is obtained from a three-level model analysis in the short-pulse limit:  $|9\rangle$  and  $|10\rangle$  are independently coupled to  $|0\rangle$  by a linearly polarized laser pulse with a Dirac-delta-function-like envelope. The polarization unit vector of the pulse is chosen in two ways,  $\mathbf{e}_+$  or  $\mathbf{e}_-$  defined as  $\langle 9|\hat{\mu}|0\rangle \mathbf{e}_{\pm} = \pm \langle 10|\hat{\mu}|0\rangle \mathbf{e}_{\pm}$  for each enantiomer. The directions of  $\mathbf{e}_{\pm}$  for an *R* enantiomer are illustrated in Figure 1. At the moment of irradiation ( $t = t_i$ ), the pulse with  $\mathbf{e}_+$  ( $\mathbf{e}_-$ ) produces an in-phase superposition  $|9\rangle + |10\rangle$  (out-of-phase superposition  $|9\rangle - |10\rangle$ ) in  $|\Psi(t_i)\rangle$ . At  $t > t_i$ , the electron wave packet propagates freely. Hence,  $|9\rangle \pm |10\rangle$  in  $|\Psi(t_i)\rangle$  temporally evolves as  $|9\rangle \pm e^{-i\phi(t)} |10\rangle$  except for the global phase factor, where  $\phi(t) = 2\Delta E(t - t_i)/\hbar$ .<sup>[7]</sup>  $e^{-i\phi(t)}$  changes as  $+1 \rightarrow -i \rightarrow -1 \rightarrow +i \rightarrow +1 \rightarrow \dots$  with the progression of  $t - t_i$ ,  $0 \rightarrow T/4 \rightarrow T/2 \rightarrow 3T/4 \rightarrow T \rightarrow \dots$ , where  $T \equiv \pi\hbar/\Delta E$ . This indicates that, in the first quarter period of  $T$  after

excitation,  $|\mp\rangle$  is created in an *R* enantiomer, while  $|\pm\rangle$  is created in an *S* enantiomer. The polarization direction determines the initial direction of  $\pi$ -electron rotation. Afterwards, the rotation direction switches between clockwise and counterclockwise with the period  $T$ . If a molecule is highly symmetric, e.g., benzene,  $e^{-i\phi(t)}$  takes an infinite time to reach  $-i$  since  $\Delta E = 0$ . That is, lowering the molecular symmetry is essential for the selective generation of either  $|+\rangle$  or  $|-\rangle$  by a linearly polarized laser pulse. Finally, the peak intensity  $f$  and the pulse duration  $t_d$  of  $\epsilon(t)$  are determined so that the pulse area is equal to  $\pi$ , following the idea of the so-called  $\pi$  pulse.<sup>[8]</sup>

To demonstrate this, a numerical simulation within 136-state expansion was carried out for an *R* enantiomer with a linearly polarized laser pulse  $\epsilon(t)$  designed to initially create  $|-\rangle$ . The polarization vector of the pulse is  $\mathbf{e}_+$ . Figure 2a

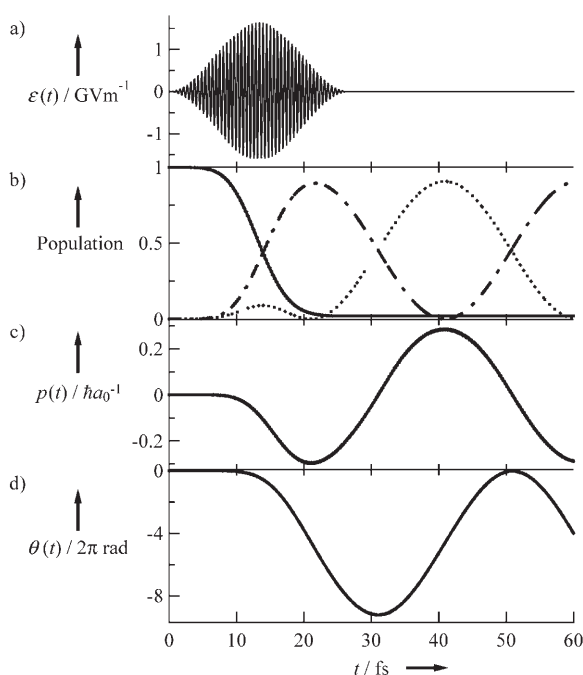


**Figure 2.** a) The linearly polarized laser pulse to initially create  $|-\rangle$  of an *R* enantiomer,  $\epsilon(t) = \mathbf{e}_+ f \sin^2(\pi t/t_d) \cos(\omega t)$  for  $0 < t < t_d$  and otherwise  $\epsilon(t) = 0$ . Here,  $\omega = 7.72 \text{ eV}/\hbar$ ,  $f = 1.63 \text{ GVm}^{-1}$ , and  $t_d = 26.6 \text{ fs}$ . b) Temporal behavior in the populations of  $|0\rangle$  (solid line),  $|+\rangle$  (dotted line), and  $|-\rangle$  (dashed-dotted line). c) Expectation value of momentum  $p(t)$ . d) Expectation value of rotational angle  $\theta(t)$ .

shows the temporal behavior in  $\epsilon(t)$ . In Figure 2b, the solid, dotted, and dashed-dotted lines denote the temporal behavior in the populations of  $|0\rangle$ ,  $|+\rangle$ , and  $|-\rangle$ , respectively. The values for  $p(t)$  and  $\theta(t)$  are plotted in Figure 2c and d, respectively. If the pulse duration  $t_d$  is less than the oscillation period  $T$ ,  $|9\rangle + |10\rangle$  is mainly produced around the pulse peak, that is,  $t_i = t_d/2 = 13.3 \text{ fs}$ . At  $t > 13.3 \text{ fs}$ , a significant amount of the population is transferred to  $|9\rangle - i|10\rangle$ , that is,  $|-\rangle$  (Figure 2b), and accordingly  $\pi$  electrons start to rotate clockwise (see Figure 1 and Figure 2c). The total population of  $\pi$  electrons in  $|+\rangle$  and  $|-\rangle$  reaches 0.908 when the laser pulse ceases at  $t = 26.6 \text{ fs}$ . From the energy–time uncertainty relation, the final value of the total population is maximum at

the pulse duration  $t_d = 26.6 \text{ fs}$ : A smaller bandwidth of a longer pulse does not cover the energy gap  $2\Delta E$  sufficiently, and, on the other hand, a broader bandwidth of a shorter pulse populates other excited states. At  $t > 26.6 \text{ fs}$ , the population of 0.908 is exchanged between  $|+\rangle$  and  $|-\rangle$  as expected.  $p(t)$  and  $\theta(t)$  thus oscillate with the period of  $T = 39.5 \text{ fs}$ , and  $\pi$  electrons are estimated to circulate around the ring more than nine times within this period (Figure 2d).

The three-level model analysis in a short-pulse limit also provides a clue to a simple control method for determining unidirectional rotation of  $\pi$  electrons: The population created in  $|-\rangle$  can be dumped to  $|0\rangle$  by applying a dump pulse with  $\mathbf{e}_-$  just after the population has completely shifted to  $|9\rangle - |10\rangle$ . Figure 3 shows the results of a pump–dump control simulation

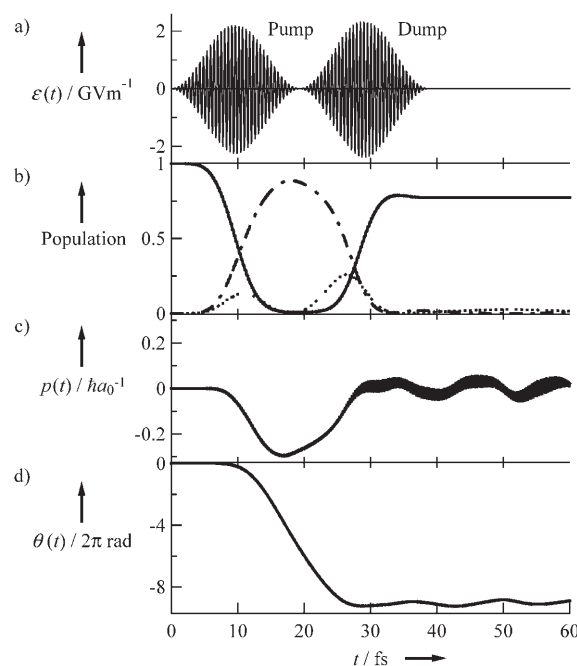


**Figure 3.** a) Pump and dump pulses for clockwise rotation of  $\pi$ -electrons in an *R* enantiomer. The polarization vectors of the pump and dump pulses are  $\mathbf{e}_+$  and  $\mathbf{e}_-$ , respectively. For the pump pulse,  $\omega = 7.72 \text{ eV}/\hbar$ ,  $f = 2.24 \text{ GVm}^{-1}$ ,  $t_d = 19.4 \text{ fs}$ ; for the dump pulse,  $\omega = 7.72 \text{ eV}/\hbar$ ,  $f = 2.37 \text{ GVm}^{-1}$ ,  $t_d = 19.4 \text{ fs}$ . The delay time between the pulses is 19.4 fs. b) Temporal behavior in the populations of  $|0\rangle$  (solid line),  $|+\rangle$  (dotted line), and  $|-\rangle$  (dashed-dotted line). c) Expectation value of momentum  $p(t)$ . d) Expectation value of rotational angle  $\theta(t)$ .

of an *R* enantiomer, which were obtained within 136-state expansion. Around the peak of the dump pulse at  $t = 29.1 \text{ fs}$ , the populations of  $|+\rangle$  and  $|-\rangle$  are nearly equal; in other words, an out-of-phase superposition  $|9\rangle - |10\rangle$  is created (Figure 3b). At  $t > 29.1 \text{ fs}$ , most of the population is dumped to  $|0\rangle$ ; the rest is brought to higher excited states. Consequently, the value of  $p(t)$  is almost zero, and reverse rotation is successfully prevented (Figure 3c and d). A pair of pump and dump pulses realizes unidirectional rotation of  $\pi$  electrons. Moreover, repetition of the unidirectional rotation can be achieved by a sequence of pulse pairs.

$\pi$ -Electron rotation in an *S* enantiomer can be controlled in the same way. By reversing the polarization directions of

the pump and dump pulses for an *R* enantiomer with respect to a reflection plane,  $\pi$  electrons in an *S* enantiomer are rotated counterclockwise in Figure 1.

$\pi$ -Electron rotation controlled by linearly polarized laser pulses may be detected experimentally using attosecond time-resolved photoelectron spectroscopy. Electron dynamics in molecules or ions are now analyzed using photoelectron-imaging techniques in an attosecond time regime.<sup>[9,10]</sup> The results of a theoretical study on  $\pi$ -electron rotation in photoelectron spectra of chiral aromatic molecules will be reported elsewhere.

In conclusion, we have presented the theoretical foundations of switching on and off photocurrents in chiral systems. By means of quantum mechanical simulation within a semi-empirical molecular orbital theory, we have shown that  $\pi$  electrons can be rotated along the ring of a chiral aromatic molecule using a single-color linearly polarized laser pulse.  $\pi$ -Electron rotation originates from creation of an (approximate) angular momentum eigenstate consisting of optically allowed, quasi-degenerate  $\pi$ -electronic excited states. Lowering the molecular symmetry is crucial for the selective generation of one of the approximate eigenstates. The rotation direction depends on the polarization direction of the applied pulse. Unidirectional rotation of  $\pi$  electrons can be performed by pump and dump pulses whose polarization directions are properly chosen. By adjusting the alignments of *S* and *R* enantiomers relative to the polarization directions, it is possible to produce photoinduced ring currents in opposite directions or a photoinduced ring current in only one of the enantiomers. Optical control of  $\pi$ -electron motions in a large, three-dimensional system, such as fullerene derivatives, is one of the challenging targets for further applications.

Received: June 28, 2006

Revised: August 2, 2006

Published online: November 3, 2006

**Keywords:** chirality · electron dynamics · laser chemistry · ring currents

- [1] P. Krause, T. Klamroth, P. Saalfrank, *J. Chem. Phys.* **2005**, *123*, 074105.
- [2] M. F. Kling, C. Siedschlag, A. J. Verhoeve, J. I. Khan, M. Schultze, T. Uphues, Y. Ni, M. Uiberacker, M. Drescher, F. Krausz, M. J. J. Vrakking, *Science* **2006**, *312*, 246.
- [3] I. Barth, J. Manz, *Angew. Chem.* **2006**, *118*, 3028; *Angew. Chem. Int. Ed.* **2006**, *45*, 2962; I. Barth, J. Manz, Y. Shigeta, K. Yagi, *J. Am. Chem. Soc.* **2006**, *128*, 7043.
- [4] S. Abe, J. Yu, W. P. Su, *Phys. Rev. B* **1992**, *45*, 8264; V. A. Shakin, S. Abe, *Phys. Rev. B* **1994**, *50*, 4306.
- [5] M. Chandross, Y. Shimoi, S. Mazumdar, *Phys. Rev. B* **1999**, *59*, 4822; M. Suzuki, S. Mukamel, *J. Chem. Phys.* **2003**, *119*, 4722.
- [6] A. Streitwieser, Jr., *Molecular Orbital Theory for Organic Chemists*, Wiley, New York, **1961**, p. 117.
- [7] See Supporting Information for this communication.
- [8] B. W. Shore, *The Theory of Coherent Atomic Excitation, Vol. 1*, Wiley, New York, **1990**, p. 304.
- [9] J. Itatani, J. Levesque, D. Zeidler, H. Niikura, H. Pépin, J. C. Kieffer, P. B. Corkum, D. M. Villeneuve, *Nature* **2004**, *432*, 867.
- [10] G. L. Yudin, A. D. Bandrauk, P. B. Corkum, *Phys. Rev. Lett.* **2006**, *96*, 063002.